Chapter 16

Advanced Imaging Methods: WIPE

Eric Anterrieu

Eric.Anterrieu@obs-mip.fr

Observatoire Midi-Pyrénées – UMR5572, 14, avenue Edouard Belin, F-31400 Toulouse, France

16.1 Introduction

This lecture is the second part of a series describing how the visibility samples provided by an interferometric device can be used to produce a high quality image of the sky.

WIPE is a regularized Fourier synthesis method recently developed in radio imaging and optical interferometry. The name of WIPE is associated with that of CLEAN, the well-known deconvolution method presented in the previous lecture, and intensively used by astronomers at IRAM as well as in many institutes, worldwide.

The regularization principle of WIPE refers to the Shannon sampling formula and to theoretical considerations related to multiresolution analysis. The notions of field and resolution appear via the definition of two key spaces: the *object space* and the *object representation space* (a subspace of the first). The complex visibilities define a function in another space: the *data space*. The functions lying in this space take their values on a frequency list which is the concatenation of the *experimental frequency list* and a *regularization frequency list*. The latter defines a virtual frequency coverage beyond the *frequency coverage to be synthesized*, up to the highest frequencies of the *scaling functions* generating the *object space*. This virtual sampling is performed at the Shannon rate corresponding to the synthesized field. The reconstructed image, also called the *neat map*, is defined as the function minimizing a regularized objective functional in which the data are damped appropriately. To describe WIPE we adopt a terminology derived from that of CLEAN.

In this lecture, we present the basic foundations of WIPE, and its implementation in the IRAM data processing software. The reader interested in the theoretical aspects and developments of WIPE is invited to consult the articles [Lannes et al. 1994], [Lannes et al. 1996], [Lannes et al. 1997].

16.2   Object space

In the problems of Fourier synthesis encountered in astronomy, the *object function* of interest, Φ_o, is a real-valued function of an angular position variable $\boldsymbol{\sigma} \equiv \boldsymbol{x} = (x, y)$. The geometrical elements under consideration are presented in Fig. 16.1.
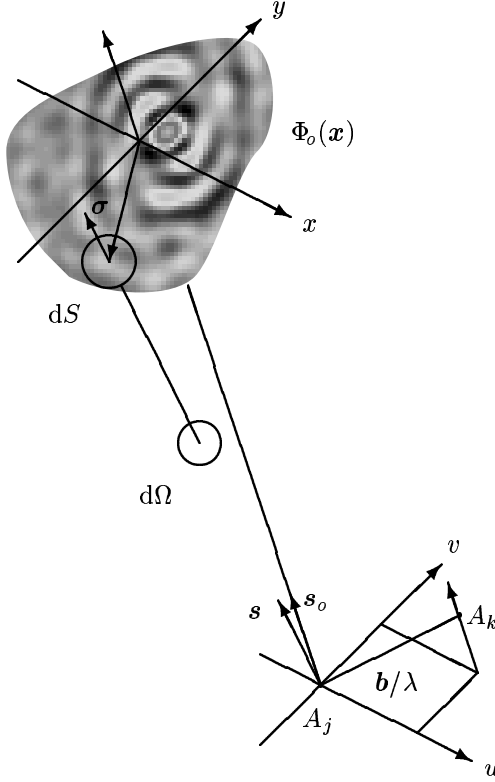

Figure 16.1: Traditional coordinate systems used to express the relation between the complex visibilities and the brightness distribution of a source under observation. Here, the two antennas A_j and A_k point toward a distant radio source in a direction indicated by the unit vector $\boldsymbol{s}$, and $\boldsymbol{b}$ is the interferometer baseline vector. The position pointed by the unit vector $\boldsymbol{s}_o$ is commonly referred to as the *phase tracking center* or *phase reference position*: $\boldsymbol{s} - \boldsymbol{s}_o = \boldsymbol{\sigma}$.

The *object model variable* ϕ lies in some *object space* H_o whose vectors, the functions ϕ, are defined at a high level of resolution. This space is characterized by two key parameters: the extension Δx of its field, and its resolution scale δx. To define this *object space* more explicitly, we first introduce the finite grid (see Fig. 16.2):

$$\boldsymbol{G} = \boldsymbol{L} \times \boldsymbol{L}, \quad \boldsymbol{L} = \left\{ p \in \boldsymbol{Z} : -\frac{N}{2} \leq p \leq \frac{N}{2} - 1 \right\}, \tag{16.1}$$

where N is some power of 2.

On each *pixel* $\boldsymbol{p}\,\delta x (\boldsymbol{p} \in \boldsymbol{G})$, we then center a *scaling function* of the form

$$e_{\boldsymbol{p}}(\boldsymbol{x}) = e_{\boldsymbol{0}}(\boldsymbol{x} - \boldsymbol{p}\,\delta x) \quad \text{with} \quad e_{\boldsymbol{0}}(\boldsymbol{x}) = \operatorname{sinc}\left(\frac{x}{\delta x}\right)\operatorname{sinc}\left(\frac{y}{\delta x}\right). \tag{16.2}$$

It is easy to verify that these functions form an orthogonal set. In this presentation of WIPE, the *object space* H_o is the Euclidian space generated by the basis vectors $e_{\boldsymbol{p}}$, $\boldsymbol{p}$ spanning $\boldsymbol{G}$ (see Fig. 16.2).
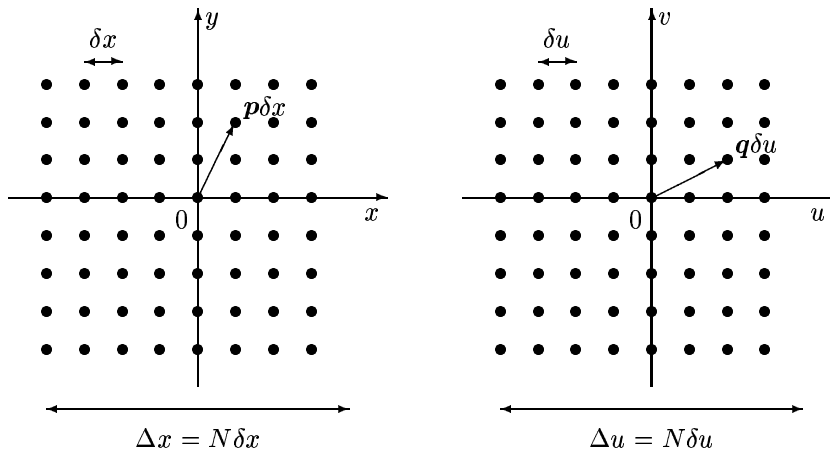
Figure 16.2: Object grid $\boldsymbol{G}\,\delta x$ *(left hand)* and Fourier grid $\boldsymbol{G}\,\delta u$ *(right hand)* for $N = 8$. The object domain is characterized by its resolution scale δx and the extension of its field $\Delta x = N\delta x$, where N is some power of 2 (the larger is N, the more oversampled is the object field). The basic Fourier sampling interval is $\delta u = 1/\Delta x$, the extension of the Fourier domain is $\Delta u = 1/\delta x$.

The dimension of this space is equal to N^2: the number of *pixels* in the grid $\boldsymbol{G}$. The functions ϕ lying in H_o can therefore be expanded in the form

$$\phi(\boldsymbol{x}) = \sum_{\boldsymbol{p}\in\boldsymbol{G}} a_{\boldsymbol{p}} e_{\boldsymbol{p}}(\boldsymbol{x}), \tag{16.3}$$

where the $a_{\boldsymbol{p}}$'s are the components of ϕ in the interpolation basis of H_o.

The Fourier transform of ϕ is defined by the relationship

$$\widehat{\phi}(\boldsymbol{u}) = \int \phi(\boldsymbol{x})\,\mathrm{e}^{-2\mathrm{i}\pi\boldsymbol{u}\cdot\boldsymbol{x}}\,\mathrm{d}\boldsymbol{x},$$

where $\boldsymbol{u}$ is a two-dimensional angular spatial frequency: $\boldsymbol{u} = (u, v)$. According to the expansion of ϕ we therefore have:

$$\widehat{\phi}(\boldsymbol{u}) = \sum_{\boldsymbol{p}\in\boldsymbol{G}} a_{\boldsymbol{p}}\widehat{e}_{\boldsymbol{p}}(\boldsymbol{u}), \tag{16.4}$$

where

$$\widehat{e}_{\boldsymbol{p}}(\boldsymbol{u}) = \widehat{e}_{\boldsymbol{0}}(\boldsymbol{u})\,\mathrm{e}^{-2\mathrm{i}\pi\boldsymbol{p}\cdot\frac{\boldsymbol{u}}{\Delta u}} \quad \text{with} \quad \widehat{e}_{\boldsymbol{0}}(\boldsymbol{u}) = \frac{1}{(\Delta u)^2}\,\mathrm{rect}\Big(\frac{u}{\Delta u}\Big)\mathrm{rect}\Big(\frac{v}{\Delta u}\Big) \tag{16.5}$$

and $\Delta u = 1/\delta x$.

The dual space of the *object space*, $\widehat{H}_o$, is the image of H_o by the Fourier transform operator: $\widehat{H}_o$ is the space of the Fourier transforms of the functions ϕ lying in H_o. This space is characterized by two key parameters: its extension $\Delta u = 1/\delta x$, and the basic Fourier sampling interval $\delta u = 1/\Delta x$ (see Fig. 16.2).

16.3 Experimental data space

The *experimental data* $\Psi_e(\boldsymbol{u})$ are blurred values of $\widehat{\Phi}_o(\boldsymbol{u})$ on a finite list of frequencies in the Fourier domain:

$$\mathcal{L}_e = \{\boldsymbol{u}_e(1), \boldsymbol{u}_e(2), \ldots, \boldsymbol{u}_e(N_e)\}. \tag{16.6}$$

As the *object function* of interest Φ_o is a real-valued function, it is natural to define $\Psi_e(-\boldsymbol{u})$ as the complex conjugate of $\Psi_e(\boldsymbol{u})$. The *experimental frequency list* $\mathcal{L}_e$ is defined consequently: if $\boldsymbol{u} \in \mathcal{L}_e$, then $-\boldsymbol{u} \in \mathcal{L}_e$ (except for the null frequency $\boldsymbol{u} = \boldsymbol{0}$: in the convention adopted here, either it does not lie in $\mathcal{L}_e$, or there exists only one occurrence of this point). The *experimental frequency coverage* generated by $\mathcal{L}_e$ is therefore centrosymmetric (see Fig. 16.3).
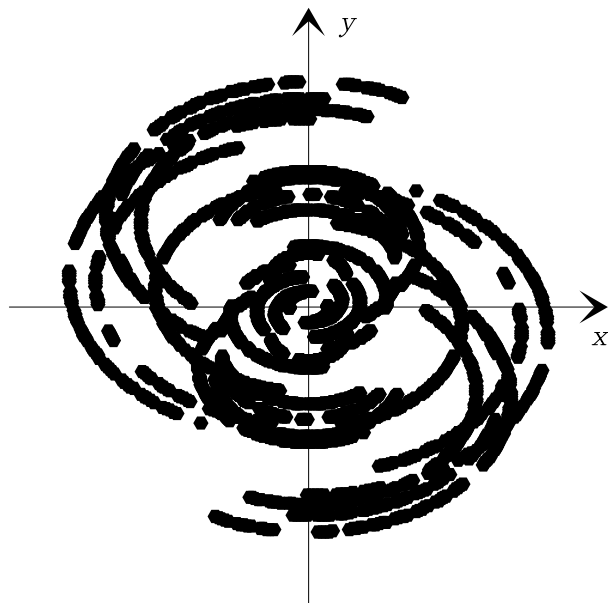

Figure 16.3: An example of an *experimental frequency coverage* provided by the IRAM interferometer. Here, the number of points N_e in the *experimental frequency list* $\mathcal{L}_e$ is equal to 2862.

The *experimental data* vector Ψ_e lies in the *experimental data space* K_e, the real Euclidian space underlying the space of complex-valued functions ψ on $\mathcal{L}_e$, such that $\psi(-\boldsymbol{u}) = \bar{\psi}(\boldsymbol{u})$. The dimension of this space is equal to N_e: the number of points in the *experimental frequency list* $\mathcal{L}_e$.

16.4   Image reconstruction process

As the *experimental frequency list* is finite, and in addition the *experimental data* blurred, the object representation that can be obtained from these data is of course incomplete. This simple remark shows that the inverse problems of Fourier synthesis must be regularized: the high-frequency components of the *image to be reconstructed* must be negligible.

The central problem is to specify in which conditions it is possible to extrapolate or interpolate, in some region of the Fourier domain, the Fourier transform of a function ϕ whose support is contained in some finite region of H_o. It is now well established that extrapolation is forbidden, and interpolation allowed to a certain extent. The corresponding regularization principle is then intimately related to the concept of resolution: the interpolation is performed in the frequency gaps of the *frequency coverage to be synthesized*.

16.4.1   Synthesized aperture

Let $\mathcal{H}$ be the Fourier domain: $\mathcal{H} = (-\Delta u/2, \Delta u/2)^2$. In Fourier synthesis, the *frequency coverage to be synthesized* is a centro-symmetric region $\mathcal{H}_s \subset \mathcal{H}$ (see Fig. 16.4).

CLEAN and WIPE share a common objective, that of the *image to be reconstructed*. This image, Φ_s, is defined so that its Fourier transform is quadratically negligible outside $\mathcal{H}_s$. More explicitly, Φ_s is defined by the convolution relation:

$$\Phi_s = \Theta_s \star \Phi_o. \tag{16.7}$$

The "synthetic beam" Θ_s is a function resulting from the choice of $\mathcal{H}_s$: the well-known *clean beam* in CLEAN, the *neat beam* in WIPE.

16.4.2 Synthetic beam

The *neat beam* can be regarded as a sort of optimal *clean beam*: the optimal apodized point-spread function that can be designed within the limits of the Heisenberg principle. More precisely, the *neat beam* Θ_s is a centro-symmetric function lying in the *object space* H_o, and satisfying the following properties:

- The energy of $\widehat{\Theta}_s$ is concentrated in $\mathcal{H}_s$. In other words, $\widehat{\Theta}_s$ has to be small outside $\mathcal{H}_s$ in the mean-square sense: we impose the fraction χ^2 of this energy in $\mathcal{H}_s$ to be close to 1 (say $\chi^2 = 0.98$).

- The effective support $\mathcal{D}_s$ of Θ_s in H_o is as small as possible with respect to the choice of $\mathcal{H}_s$ and χ^2. The idea is of course to have the best possible resolution.

This apodized point-spread function is thus computed on the grounds of a trade-off between resolution and efficiency, with the aid of the *power method*.
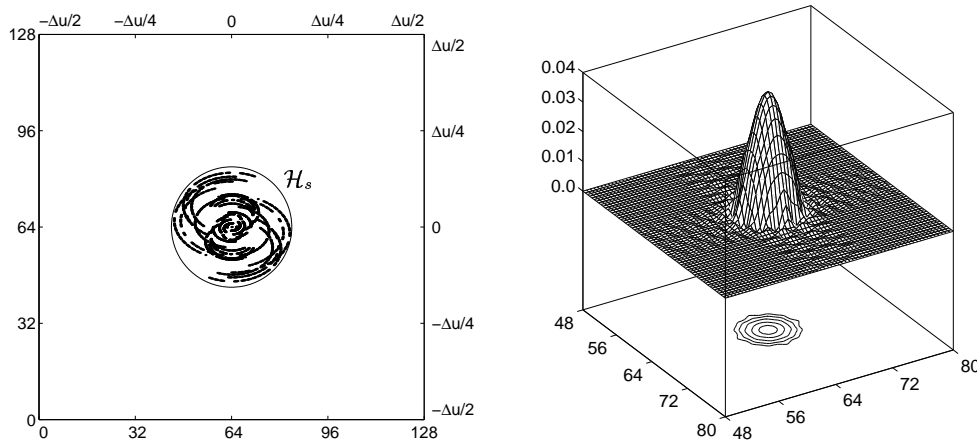

Figure 16.4: *Experimental frequency coverage* and *frequency coverage to be synthesized $\mathcal{H}_s$ (left hand).* The *experimental frequency list $\mathcal{L}_e$* includes $N_e = 2862$ frequency points. The *frequency coverage to be synthesized $\mathcal{H}_s$* is centred in the Fourier grid $\boldsymbol{G}\,\delta u$, where $\delta u = \Delta u/N$ with $N = 128$ (here, the diameter of the circle is equal to $40\,\delta u$). The *neat beam Θ_s (right hand)* represented here corresponds to the *frequency coverage to be synthesized $\mathcal{H}_s$* for a given value of $\chi^2 = 0.97$. It is centred in the object grid $\boldsymbol{G}\,\delta x$ where $\delta x = 1/\Delta u$ (here, the full width of Θ_s at half maximum is equal to $5\,\delta x$).

16.4.3 Regularization frequency list

As extrapolation is forbidden, and interpolation only allowed to a certain extent in the frequency gaps of the *frequency coverage to be synthesized*, the *experimental frequency list $\mathcal{L}_e$* should be completed by high-frequency points. These points, located outside the *frequency coverage to be synthesized $\mathcal{H}_s$*, are those for which the high-frequency components of the *image to be reconstructed* are practically negligible.

The elements of the *regularization frequency list $\mathcal{L}_r$* are the frequency points $\boldsymbol{u}_r$ located outside the *frequency coverage to be synthesized $\mathcal{H}_s$* at the nodes of the Fourier grid $\boldsymbol{G}\,\delta u$:

$$\mathcal{L}_r = \{\boldsymbol{u}_r = \boldsymbol{q}\,\delta u, \boldsymbol{q} \in \boldsymbol{G} : \boldsymbol{q}\,\delta u \notin \mathcal{H}_s\}. \tag{16.8}$$

The *global frequency list $\mathcal{L}$* is then the concatenation of $\mathcal{L}_e$ with $\mathcal{L}_r$.

16.4.4   Data space

According to the definition of the *image to be reconstructed*, the Fourier data corresponding to Φ_s are defined by the relationship:

$$\Psi_s(\boldsymbol{u}) = \widehat{\Theta}_s(\boldsymbol{u})\Psi_e(\boldsymbol{u}) \quad \forall \boldsymbol{u} \in \mathcal{L}_e. \tag{16.9}$$

Clearly, Ψ_s lies in the *experimental data space* K_e.

Let us now introduce the *data vector*:

$$\Psi_d(\boldsymbol{u}) = \begin{cases} \Psi_s(\boldsymbol{u}) & \text{on } \mathcal{L}_e; \\ 0 & \text{on } \mathcal{L}_r. \end{cases} \tag{16.10}$$

This vector lies in the *data space* K_d, the real Euclidian space underlying the space of complex-valued functions ψ on $\mathcal{L}$, such that $\psi(-\boldsymbol{u}) = \bar{\psi}(\boldsymbol{u})$. This space is equipped with the scalar product:

$$(\psi_1 \mid \psi_2)_d = \sum_{\boldsymbol{u} \in \mathcal{L}_e} \bar{\psi}_1(\boldsymbol{u})\psi_2(\boldsymbol{u})W(\boldsymbol{u})(\delta u)^2 + \sum_{\boldsymbol{u} \in \mathcal{L}_r} \bar{\psi}_1(\boldsymbol{u})\psi_2(\boldsymbol{u})(\delta u)^2; \tag{16.11}$$

$W(\boldsymbol{u})$ is a given *weighting function* that takes into account the reliability of the data via the standard deviation $\sigma_e(\boldsymbol{u})$ of $\Psi_e(\boldsymbol{u})$, as well as the local redundancy $\rho(\boldsymbol{u})$ of $\boldsymbol{u}$ up to the sampling interval δu.

The *Fourier sampling operator* A is the operator from the *object space* H_o into the *data space* K_d:

$$A : H_o \longrightarrow K_d, \qquad (A\phi)(\boldsymbol{u}) = \begin{cases} \widehat{\phi}(\boldsymbol{u}) & \text{on } \mathcal{L}_e; \\ \widehat{\phi}(\boldsymbol{u}) & \text{on } \mathcal{L}_r. \end{cases} \tag{16.12}$$

As the *experimental data* $\Psi_e(\boldsymbol{u})$ are blurred values of $\widehat{\Phi}_o(\boldsymbol{u})$ on $\mathcal{L}_e$, this operator will play a key role in the image reconstruction process. The definition of this *Fourier sampling operator* suggests that the action of A should be decomposed into two components: A_e on the *experimental frequency list* $\mathcal{L}_e$, and A_r on the *regularization frequency list* $\mathcal{L}_r$.

16.4.5   Object representation space

The *reconstructed image* is defined as the function Φ_E of the *object space* H_o minimizing some objective functional. The definition of this functional takes into account the nature of the data, as well as other constraints. For example, the *image to be reconstructed* may be confined to a subspace, or more generally to a convex set, of the *object space* H_o: this convex set is the *object representation space* E. It may be defined from the outset (in an interactive manner, for example), or step by step throughout the image reconstruction procedure (this is the case of the current implementation of WIPE). In both cases, the projection operator onto this space, the projector P_E, will play an essential role in the image reconstruction process.

REMARK 1: positivity constraint.

In most cases encountered in practice, the scalar components of Φ_E in the interpolation basis of H_o must be non-negative (cf. Eq.**??**). In the current implementation of WIPE this constraint is taken into account. The *object representation space* E is then built, step by step, accordingly.

16.4.6   Objective functional

The *reconstructed image* is defined as the function Φ_E minimizing on E the objective functional:

$$q(\phi) = \|\Psi_d - A\phi\|_d^2. \tag{16.13}$$

According to the definition of the *data vector* Ψ_d and to that of the *Fourier sampling operator* A, this quantity can be written in the form:

$$q(\phi) = q_e(\phi) + q_r(\phi) \text{ with } \begin{cases} q_e(\phi) = \displaystyle\sum_{\boldsymbol{u} \in \mathcal{L}_e} |\Psi_s(\boldsymbol{u}) - \widehat{\phi}(\boldsymbol{u})|^2 W(\boldsymbol{u})(\delta u)^2; \\ q_r(\phi) = \displaystyle\sum_{\boldsymbol{u} \in \mathcal{L}_r} |\widehat{\phi}(\boldsymbol{u})|^2 (\delta u)^2. \end{cases} \tag{16.14}$$

The experimental criterion q_e constraints the *object model* ϕ to be consistent with the damped Fourier data Ψ_s, while the regularization criterion q_r penalizes the high-frequency components of ϕ.

Let now F be the image of E by A (the space of the $A\phi$'s, ϕ spanning E), A_E be the operator from E into F induced by A, and Ψ_F the projection of Ψ_d onto F (see Fig. 16.7). The vectors ϕ minimizing q on E, the solutions of the problem, are such that $A_E\phi = \Psi_F$. They are identical up to a vector lying in the kernel of A_E (by definition, the kernel of A_E is the space of vectors ϕ such that $A_E\phi = 0$).

As $\Psi_d - \Psi_F$ is orthogonal to F, the solutions ϕ of the problem are characterized by the property: $\forall \varphi \in E, (A\varphi \mid \Psi_d - A\phi)_d = 0$. On denoting by A^* the adjoint of A, this property can also be written in the form:

$$\forall \varphi \in E, \quad (\varphi \mid r)_o = 0, \text{ with } r = A^*(\Psi_d - A\phi). \tag{16.15}$$

where r is regarded as a residue. This condition is of course equivalent to $P_E r = 0$, where P_E is the projector onto the *object representation space* E. The solutions of the problem are therefore the solutions of the *normal equation* on E:

$$A_E^* A_E \phi = A_E^* \Psi_d, \tag{16.16}$$

where $A_E^* = P_E A^*$.

Many different techniques can be used for solving the *normal equation* (or minimizing q on E). Some of these are certainly more efficient than others, but this is not a crucial choice.

REMARK 2: beams and maps.

The action of A^*A involved in $A_E^* A_E$ is that of a convolutor. As the two lists $\mathcal{L}_e$ and $\mathcal{L}_r$ are disjoints, we have: $A^*A = A_e^* A_e + A_r^* A_r$. Thus, the corresponding point-spread function, called the *dusty beam*, has two components: the traditional *dirty beam* Θ_d and the *regularization beam*. The latter corresponds to the action of $A_r^* A_r$, the former to that of $A_e^* A_e$ (see Fig. 16.5). Likewise, according to the definition of the *data vector*, $A^*\Psi_d = A_e^*\Psi_s$ is called the *dusty map* (as opposed to the traditional *dirty map* $A_e^*\Psi_d$ because it is damped by the *neat beam*).

REMARK 3: construction of the *object representation space*.

With regard to the construction of the *object representation space* E, CLEAN and WIPE are very similar: it is defined through the choice of the (discrete) object support. It is important to note that this space may be constructed, in a global manner or step by step, interactively or automatically. In the last version of WIPE implemented at IRAM, the image reconstruction process is initialized with a few iterations of CLEAN. The support selected by CLEAN is refined throughout the iterations of WIPE by conducting a matching pursuit process at the level of the components of r in the interpolation basis of H_o: the current support is extended by adding the nodes of the object grid $\boldsymbol{G}\,\delta x$ for which these coefficients are the largest above a given threshold (half of the maximum value, for example). The objective functional is then minimized on that new support, and the global residue r updated accordingly. The *object representation space* of the *reconstructed image* is thus obtained step by step in a natural manner.

The simulation presented on Fig.16.5-16.6 corresponds to the conditions of Fig. 16.4. The Fourier data Ψ_e were blurred by adding a Gaussian noise: for all $\boldsymbol{u} \in \mathcal{L}_e$, the standard deviation of $\Psi_e(\boldsymbol{u})$ was set equal to 5% of the total flux of the object $(\widehat{\Phi}_o(\boldsymbol{0})/20)$. The image reconstruction process was initialized with a few iterations of CLEAN, and the construction of the final support of the *reconstructed image* was made as indicated in Remark 3. At the end of the reconstruction process, a final smoothing of the current object support was performed. In this classical operation of mathematical morphology, the effective support of Θ_s, $\mathcal{D}_s$, is of course used as a structuring element. The boundaries of the effective support of the reconstructed *neat map* are thus defined at the appropriate resolution. In particular, the connected entities of size smaller than that of $\mathcal{D}_s$ are eliminated.

16.4.7 Uniqueness and robustness

When the problem is well-posed, A_E is a one-to-one map ($\ker A_E = \{0\}$) from E onto F; the solution is then unique: there exists only one vector $\phi \in E$ such that $A_E\phi = \Psi_F$. This vector, Φ_E, is said to be the least-squares solution of the equation $A_E\phi$ "$=$" Ψ_d.
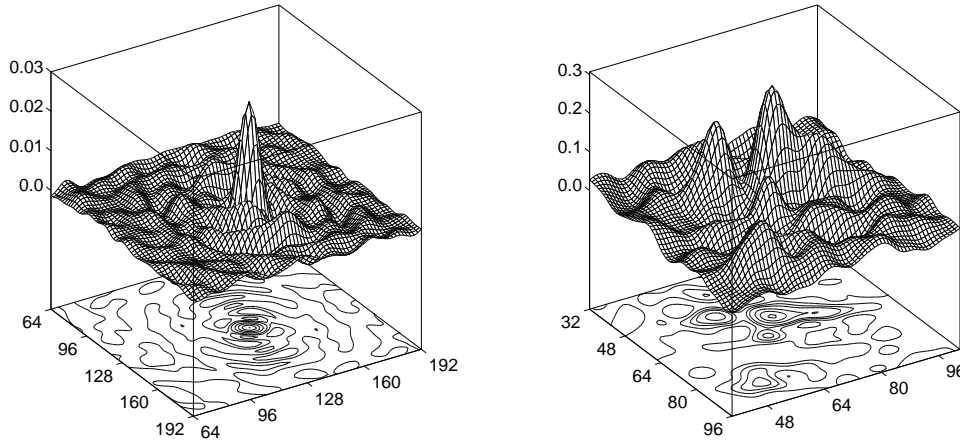
Figure 16.5: *Dirty beam (left hand)* corresponding to the *experimental frequency list* $\mathcal{L}_e$ of Fig. 16.4, and *dusty map (right hand)* of a simulated data set (the simulated Fourier data Ψ_e were blurred by adding a Gaussian noise with a standard deviation σ_e equal to 5% of the total flux of the object Φ_o).
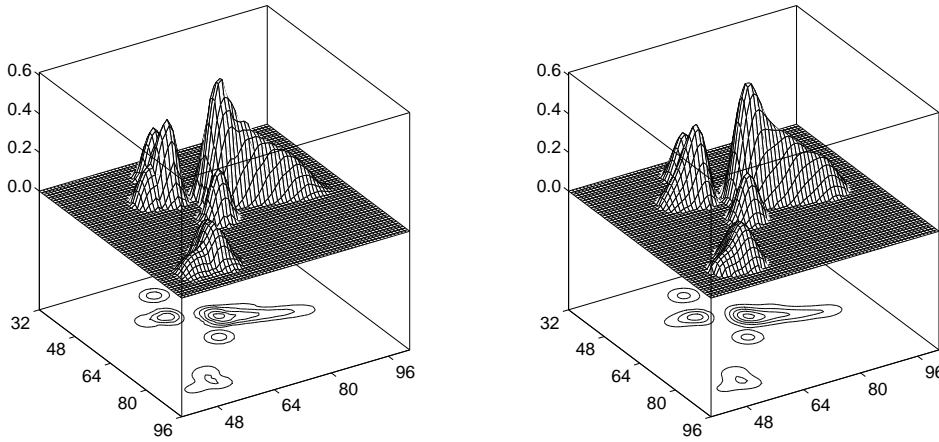

Figure 16.6: *Image to be reconstructed Φ_s (left hand)* at the resolution level defined in Fig. 16.4, and reconstructed *neat map Φ_E (right hand)* at the same resolution: the final *condition number κ_E* is equal to 2.46 (cf. Eq. 16.17 and 16.18).

In this case, let $\delta\Psi_F$ be a variation of Ψ_F in F, and $\delta\Phi_E$ be the corresponding variation of Φ_E in E (see Fig. 16.7). It is easy to show that the robustness of the reconstruction process is governed by the inequality:

$$\frac{\|\delta\Phi_E\|_o}{\|\Phi_E\|_o} \leq \kappa_E \frac{\|\delta\Psi_F\|_d}{\|\Psi_F\|_d}. \tag{16.17}$$

The error amplifier factor κ_E is the condition number of A_E:

$$\kappa_E = \frac{\sqrt{\lambda'}}{\sqrt{\lambda}}; \tag{16.18}$$

here λ and λ' respectively denote the smallest and the largest eigenvalues of $A_E^* A_E$. The closer to 1 is the condition number, the easier and the more robust is the reconstruction process (see Fig. 16.8 and 16.9).

The part played by inequality 16.17 in the development of the corresponding error analysis shows that a good reconstruction procedure must also provide, in particular, the condition number κ_E. This is the
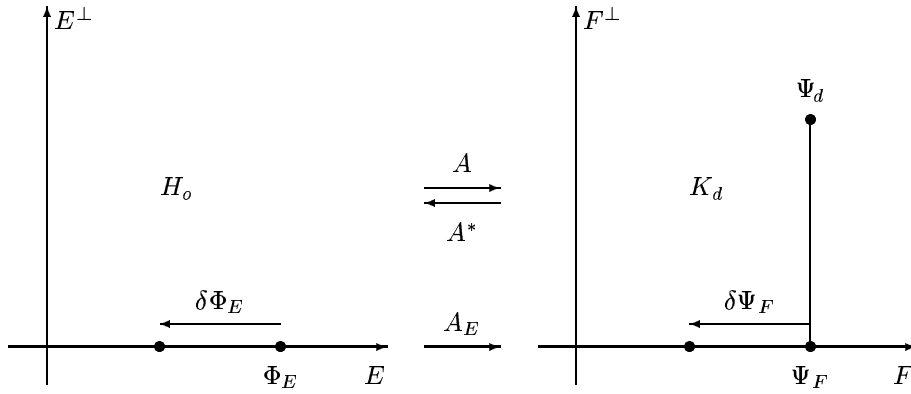
Figure 16.7: Uniqueness of the solution and robustness of the reconstruction process. Operator A is an operator from the *object space H_o* into the *data space K_d*. The *object representation space E* is a particular subspace of H_o. The image of E by A, the range of A_E, is denoted by F. In this representation, Ψ_F is the projection of the data vector Ψ_d onto F. The inverse problem must be stated so that A_E is a one-to-one map from E onto F, the condition number κ_E having a reasonable value.

case of the current implementation of WIPE which uses the *conjugate gradient* method for solving the *normal equation* 16.16.

To conduct the final error analysis, one is led to consider the eigenvalue decomposition of $A_E^* A_E$. This is done, once again, with the aid of the *conjugate gradient* method associated with the QR algorithm. At the cost of some memory overhead (that of the M successive residues), the latter also yields approximations of the eigenvalues λ_k of $A_E^* A_E$. It is thus possible to obtain the scalar components of the associated eigenmodes Φ_k in the interpolation basis of H_o. The purpose of this analysis is to check whether some of them (in particular those corresponding to the smallest eigenvalues) are excited or not in Φ_E. If so, the corresponding details may be artefacts of the reconstruction.

The reconstructed map is then decomposed in the form:

$$\Phi_E = \sum_{k=1}^{M} w_k \Phi_k, \quad w_k = (\Phi_k \mid \Phi_E). \tag{16.19}$$

The separation angle θ_k between Φ_E and Φ_k is explicitly given by the relationship:

$$\cos \theta_k = \frac{w_k}{\sqrt{\sum_{k=1}^{M} w_k^2}} \quad (0 \le \theta_k \le \pi/2). \tag{16.20}$$

The closer to $\pi/2$ is θ_k, the less excited is the corresponding eigenmode Φ_k in the reconstructed *neat map* Φ_E.

To illustrate in a concrete manner the interest of equations 16.19 and 16.20, let us consider the simulations presented in Fig. 16.4 and 16.9. Whatever the value of the final condition number is, the error analysis allows the astronomer to check if there exists a certain similitude between some details in the *neat map* and some features of the critical eigenmodes. This information is very attractive, in particular when the resolution of the reconstruction process is greater than a reasonable value (the larger is the *aperture to be synthesized $\mathcal{H}_s$*, the smaller is the full width at half-maximum of Θ_s). In such situations of "super resolution," the error analysis will suggest the astronomer to redefine the problem at a lower level of resolution, or to keep in mind that some details in the reconstructed *neat map* may be artefacts of the reconstruction process.
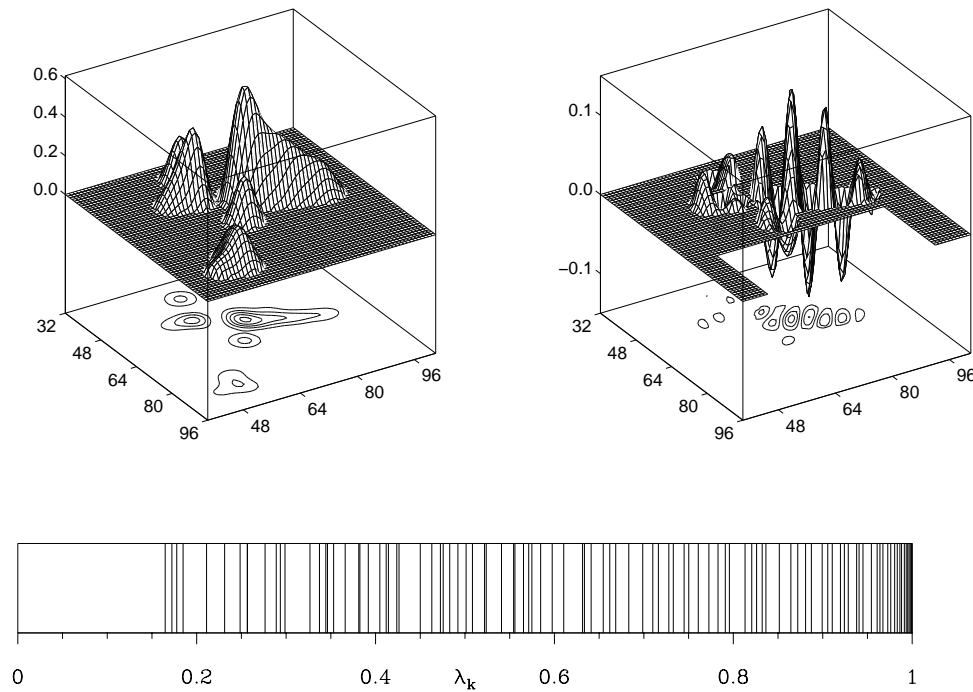
Figure 16.8: Reconstructed *neat map* Φ_E *(left hand)* and eigenmode Φ_1 *(right hand)* corresponding to the smallest eigenvalue $\lambda_1 = 0.165$ of $A_E^* A_E$. The conditions of the simulations are those of Fig. 16.4 and 16.5: in particular, the diameter of $\mathcal{H}_s$ is equal to $40\,\delta u$. The final condition number is $\kappa_E = 2.46$ (the eigenvalues of $A_E^* A_E$ are plotted on the bar code below). This eigenmode is not excited in Φ_E: the separation angle θ_1 between Φ_E and Φ_1 is greater than 89°. In other situations, when the final condition number is greater, this mode may be at the origin of some artefacts in the *neat map* (see Fig. 16.9).

16.5   Implementation of WIPE at IRAM

In this section we describe the successive steps of the image reconstruction process as it is implemented now in the MAPPING program included in the IRAM software. For more information on this program, the reader is invited to read the last version of the *Mapping CookBook*.

The first step of the image reconstruction process is to define the *object space* H_o. This space is characterized by two key parameters: the extension Δx of its field, and its resolution scale $\delta x = \Delta x/N$ (see Fig. 16.2). The procedure `wipe_init` is used to set these parameters properly.

The *frequency coverage to be synthesized* $\mathcal{H}_s$ is defined with the aid of the procedure `wipe_aper`. This tool provides an interactive way of fitting an ellipse over the *experimental frequency coverage* generated by the *experimental frequency list* $\mathcal{L}_e$ (see Fig. 16.4).

Once $\mathcal{H}_s$ has been defined, the procedure `wipe_beam` is ready for computing the *neat beam* Θ_s, as well as the *dirty beam* Θ_d. The latter plays a key role in the action of the convolutor $A_E^* A_E$, while the Fourier transform of the former is involved in the definition of the *data vector* Ψ_d (cf. Eq. 16.9 and 16.10).

The last step in the image reconstruction process concerns the *neat map*. It is implemented in the `wipe_solve` command. Before the initialization of the reconstruction, the *dusty map* $A^* \Psi_d$ is computed, and an optional support can be selected (this support plays the role of the *clean box* of CLEAN). As WIPE can be slow when reconstructing large images, it can be initialized with a few CLEAN iterations to quickly build a first *object representation space* E. When switching to WIPE, the program starts by optimizing the solution provided by CLEAN with the corresponding support. Then, at each iteration of WIPE, the support grows, and for a given and fixed *object representation space* E, the *normal equation* 16.16 is solved by using the *conjugate gradient* method, which also provides the condition number κ_E of A_E. When leaving WIPE, a final smoothing of the current object support is performed, removing (through an appropriate morphological analysis) the details of the *reconstructed image* smaller than the resolution limit
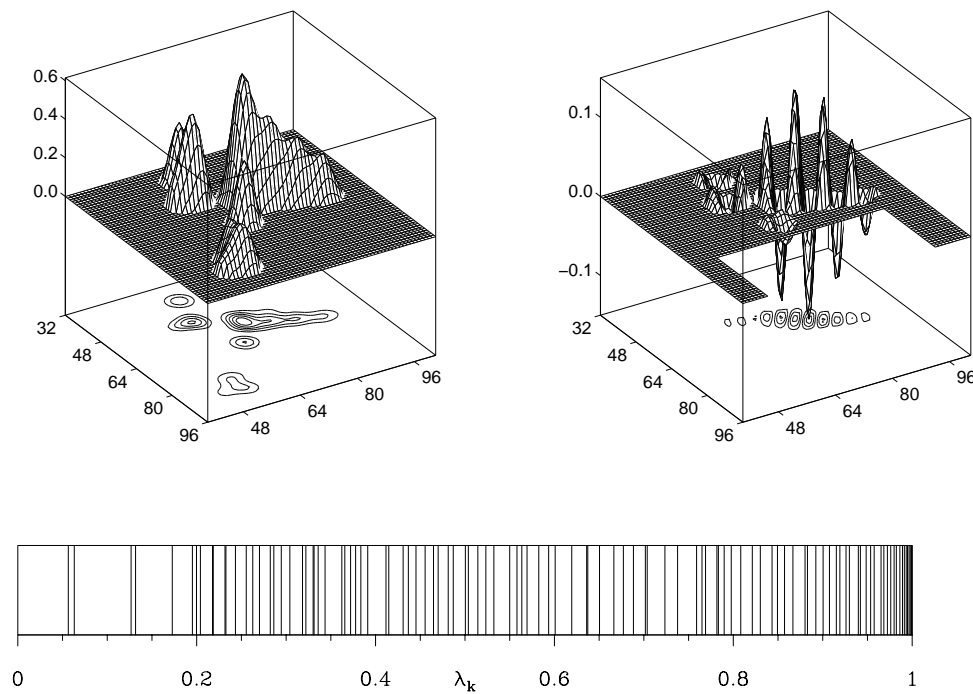
Figure 16.9: Reconstructed *neat map* Φ_E *(left hand)* and related critical eigenmode Φ_1 *(right hand)*. The latter corresponds to the smallest eigenvalue $\lambda_1 = 0.057$ of $A_E^* A_E$. The conditions of the simulations are those of Fig. 16.5, but here the diameter of $\mathcal{H}_s$ is taken equal to $48\,\delta u$: the final condition number is $\kappa_E = 4.19$ (the eigenvalues of $A_E^* A_E$ are plotted on the bar code below). The critical eigenmode Φ_1 is at the origin of the oscillations along the main structuring entity of Φ_E. This mode is slightly excited (the separation angle θ_1 between Φ_E and Φ_1 is less than $86°$), thus the corresponding details may be artefacts. In this case of "super-resolution" the error analysis provided by WIPE suggests that the procedure should be restarted at a lower level of resolution (see Fig. 16.8), so that the final solution be more stable and reliable.

of the reconstruction process. The final *reconstructed image* Φ_E is the function minimizing the objective functional 16.13 on that support.

The control of the robustness of the reconstruction process is performed through an additional step with the `wipe_error` command. This procedure computes with a fine accuracy the final *condition number* κ_E, as well as the eigenvalues and the critical eigenmodes of $A_E^* A_E$. One of the aims of this last step is to check that the features present in the *reconstructed image* are not artefacts. This can be done by comparing these features with those of the critical eigenmodes. When there exists a certain similitude (between these features), it is then recommended to restart the process with a lower resolution, so that the final solution be more stable and reliable.

Glossary

$\boldsymbol{L}, N$	One-dimensional grid, number of elements in $\boldsymbol{L}$
$\boldsymbol{G} = \boldsymbol{L} \times \boldsymbol{L}$	Two-dimensional grid
$\boldsymbol{p} = (p, q)$	Two-dimensional integer vector
$\boldsymbol{x} = (x, y)$	Two-dimensional angular position variable
$\boldsymbol{u} = (u, v)$	Two-dimensional angular spatial frequency
Δx	Extension of the synthesized field
δx	Resolution scale of the synthesized field
Δu	Extension of the Fourier domain
δu	Basic Fourier sampling interval
$\boldsymbol{G}\,\delta x, \boldsymbol{G}\,\delta u$	Object grid, Fourier grid
$\mathcal{L}$	Global frequency list
$\mathcal{L}_e, \mathcal{L}_r$	Experimental frequency list, regularization frequency list
$\mathcal{H}$	Fourier domain $[-\Delta u/2, \Delta u/2]$
$\mathcal{H}_s$	Frequency coverage to be synthesized
$\mathcal{D}_s$	Support of the neat beam Θ_s
χ^2	Energy confinement parameter
Θ_s	Apodized point-spread function (neat beam)
Θ_d	Instrumental point-spread function (dirty beam)
$H_o, e_{\boldsymbol{p}}(\boldsymbol{x})$	Object space, basis functions of H_o
E, F	Object representation space, image of E by A
K_e, K_d	Experimental data space, data space
$W(\boldsymbol{u})$	Weighting function
$\rho(\boldsymbol{u}), \sigma_e(\boldsymbol{u})$	Redundancy of $\boldsymbol{u}$, standard deviation of $\Psi_e(\boldsymbol{u})$
A	Regularized Fourier sampling operator
A_e, A_r	Fourier sampling operator on $\mathcal{L}_e$, on $\mathcal{L}_r$
P_E, A_E	Projection operator onto E, restriction of A to E
Φ_o, Φ_s	Original object function, image to be reconstructed
$\Phi_E, \delta\Phi_E$	Reconstructed image, reconstruction error on Φ_E
Ψ_e, Ψ_s	Experimental data, damped experimental data
Ψ_d	Regularized data vector
$\Psi_F, \delta\Psi_F$	Projection of Ψ_d onto F, effective error on Ψ_F
λ_k, Φ_k	Eigenvalue of $A_E^* A_E$ and related eigenmode
θ_k	Separation angle between Φ_E and Φ_k
λ, λ'	Smallest and largest eigenvalues of $A_E^* A_E$
κ_E	Condition number of A_E
$q(\phi)$	Regularized criterion
$q_e(\phi), q_r(\phi)$	Experimental criterion, regularization criterion